Structural Engineering and Mechanics, *Vol. 70, No. 4 (2019) 457-466*
DOI: https://doi.org/10.12989/sem.2019.70.4.457

Hierarchical neural network for damage detection using modal parameters

Minwoo Chang*[1], Jae Kwan Kim[2a] and Joonhyeok Lee[3b]

[1]Northern Railroad Research Center, Korea Railroad Research Institute, 176 Cheoldo bangmulgwan-ro, Uiwang-si, Gyeonggi-do 16105, Republic of Korea
[2]Department of Civil and Environmental Engineering, Seoul National University, 1 Gwanak-ro, Gwanak-gu, Seoul 08826, Republic of Korea
[3]Infrastructure ENG Team, Samsung C&T Corporation, 26 Sangil-ro 6-gil, Gangdong-gu, Seoul 05288, Republic of Korea

(Received August 28, 2018, Revised April 12, 2019, Accepted April 13, 2019)

Abstract. This study develops a damage detection method based on neural networks. The performance of the method is numerically and experimentally verified using a three-story shear building model. The framework is mainly composed of two hierarchical stages to identify damage location and extent using artificial neural network (ANN). The normalized damage signature index, that is a normalized ratio of the changes in the natural frequency and mode shape caused by the damage, is used to identify the damage location. The modal parameters extracted from the numerically developed structure for multiple damage scenarios are used to train the ANN. The positive alarm from the first stage of damage detection activates the second stage of ANN to assess the damage extent. The difference in mode shape vectors between the intact and damaged structures is used to determine the extent of the related damage. The entire procedure is verified using laboratory experiments. The damage is artificially modeled by replacing the column element with a narrow section, and a stochastic subspace identification method is used to identify the modal parameters. The results verify that the proposed method can accurately detect the damage location and extent.

Keywords: artificial neural network; damage detection; normalized damage significance index; modal identification; structural health monitoring

1. Introduction

The preliminary goal of Structural Health Monitoring (SHM) is to maintain the safety and serviceability of constructed structures by assessing their condition (Sohn *et al.* 2003, Shahidi and Pakzad 2013). Since the deterioration process of civil infrastructure is ongoing, a posteriori effort to maintain performance is necessary by conducting SHM throughout its lifetime (Chang *et al.* 2003). Upon identifying damage, management agencies must analyze the cause of the damage and prepare a suitable repair plan depending on the damage severity and scenarios (Maguire *et al.* 2018, Torres *et al.* 2018). Accordingly, SHM algorithms should be developed to generalize the damage identification procedures and to provide accurate estimation of condition states, which can assist the decision making process (Chang *et al.* 2017).

Applications for such algorithms generally use cumulatively monitored sensor data that are translated into the measures of the presence, location, and extent of possible damage (Kondo and Hamamoto 1994). Because structural damage causes stiffness reduction in structural members, the modal properties of such a dynamic structure, including the natural frequencies and mode shapes, are expected to change as a result of the damage. The sensitivity of the natural frequency has been used as an index to detect, locate, and quantify damage (Majumdar *et al.* 2013). Various damage detection methods based on modal frequency change were reviewed by Salawu (1997). In addition to natural frequencies, changes in the mode shapes have been used to detect local damages (Pandey *et al.* 1991, Ratcliffe 1997, Cornwell *et al.* 1999, Yoon *et al.* 2005, Yazdanpanah *et al.* 2015). Numerical simulations and controlled laboratory experiments have shown good agreement with regard to detection of artificial damage (Radzieński *et al.* 2011, Chen and Loh 2018).

Although the damage detection methods showed reliable results in the controlled laboratory experiments, many obstacles have been reported when they are applied to existing structures. For example, variations in temperature and traffic loading affect the structural condition more than gradual deterioration and local damage (Sohn 2007, Farreras-Alcover *et al.* 2015, Nguyen *et al.* 2016, Zolghadri *et al.* 2016). For accurate modal parameter estimation and damage detection, varying temperature conditions were investigated in a numerically simulated model, and the structural responses from the existing structure were measured for over two years (Limongelli 2010, Magalhães *et al.* 2012).

To extract damage features accurately, damage detection algorithms based on machine learning techniques have been developed (Worden and Manson 2006). Artificial neural network (ANN), a machine learning technique, imitates the

*Corresponding author, Senior Researcher
E-mail: cmw321@krri.re.kr
[a] †Deceased; formerly, Professor
[b] Manager

ISSN: 1225-4568 (Print), 1598-6217 (Online)

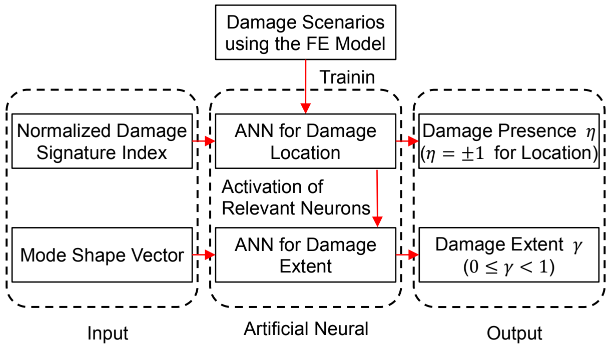

Fig. 1 Framework for damage detection using ANNs

way information is processed in a human brain and serves as a tool to recognize the varying patterns caused by damage (Wu *et al.* 1992). Owing to the recent development of sensor technologies and computing systems, a massive volume of data can be processed to train ANN algorithms. Levin and Lieven (1998) applied ANN to update a finite element (FE) model using simulated data with and without noise. ANN has been used to detect damage to various structural systems, including beam to column connections, bridges, and bearing components (Yun *et al.* 2001, Cho *et al.* 2004, Lee *et al.* 2005, Ali *et al.* 2015). Recently, the increase in the performance of computing systems has enabled processing of visual images to detect concrete cracks using convolution neural networks (Cha *et al.* 2017, Dorafshan *et al.* 2018). Hakim and Razak (2014) reviewed ANN-based damage detection algorithms, which use modal parameters as damage features.

In many studies, ANNs examine the structural conditions using modal parameters from FE models to correspond to possible damage scenarios. This process is called "training." In contrast to the modal parameters that usually provide a global feature of the structural system, detection at the element level enables identification of multiple damage information, including its presence, location, and extent (Yun *et al.* 2001). ANN algorithms are generally based on a single-stage scheme, in which numerous damage scenarios associated with both the damage location and extent are used to train the ANN algorithm. Despite the convenient use of such techniques, the single-stage scheme is computationally inefficient for the training and processing of parameters in the monitored structures (Hakim *et al.* 2011). Additionally, the single-stage scheme eventually results in a false damage alarm due to a misleading structural damage induced from minor changes in the damage indices (Lee *et al.* 2005, Bakhary *et al.* 2010). A multi-stage scheme can resolve these issues by separating the damage identification procedures into several hierarchical steps (Ko *et al.* 2002, Qu *et al.* 2003, Park *et al.* 2009).

This study presents a damage detection method using ANN, based on a two-stage scheme. The modal parameters are converted to the input for the training of each ANN. Since the modal parameters vary depending on the data investigated, it is difficult to identify the true structural modes, especially for existing structures. The modal identification technique is combined with hierarchical ANN to estimate the accurate modal information and to eliminate the noisy contribution in the measured sensor data. As a measure of the structural condition, the damage signature index (DSI) is investigated (Lam *et al.* 1998). The mathematical feature of the DSI, which is used to determine the presence of damage and its location, is that it is irrelevant to the damage extent and is only affected by the location. The difference in mode shape vectors is used to evaluate the damage extent. A three-story shear frame model is used to validate the proposed algorithm. To train the ANN, an FE model simulating a laboratory experiment is developed. The vibration data measured from the shear frame model are used to estimate the modal parameters for several damage scenarios and to validate the proposed method.

2. Damage detection using artificial neural network

The framework for the proposed damage detection algorithm using ANN is shown in Fig. 1. Two ANNs are sequentially trained for identification of the damage location and its extent. The multi-stage scheme is computationally efficient to train the damage scenarios associated with their presences, locations, and severities, with and without error contribution (Ko *et al.* 2002). For each ANN, a damage-sensitive feature is estimated to recognize the changes in the healthy state of the structure using the modal parameters from FE models associated with the intact and damaged structures. The first-stage ANN aims to determine the presence of damage and its location. Here, the normalized ratio of the changes in the modal frequency and mode shape, known as normalized DSI (NDSI), is investigated (Lam *et al.* 1998). NDSI is sensitive to damage location and independent of damage extent, which greatly reduces the number of damage scenarios required to train the ANN. The damage-positive alarm from this step transmits the associated neuron to evaluate the damage extent. The similarity in mode shape vectors from the intact and damaged structures, denoted by the modal assurance criterion (MAC), is used to train the second-stage ANN (Allemang 2003). The input for these two ANN requires the accurate estimation of modal parameters to assess the damage information of existing structures. This section briefly describes the theoretical backgrounds of the ANN, NDSI, and modal identification technique used in this study.

2.1 ANN for damage detection

ANN is composed of input, output, and hidden layers. An important feature of the human brain, namely its ability to process a considerable amount of information in parallel, is imitated by the ANN technology. Thus, the neurons in each layer are connected to multiple neurons in other layers (Fig. 2). In this study, the supervised learning rule is used to train the ANN, wherein the feedforward operation and learning processes are utilized. To train the ANN for identification of damage location and extent, a single-stage scheme is generally used.

In the feedforward operation, the training pattern for the

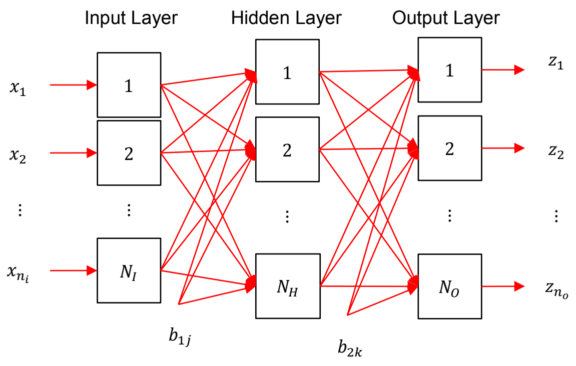

Fig. 2 ANN structure with a single hidden layer

input layer is determined and used to calculate the output y_i as follows:

$$v_i = \sum_{j=1}^{m} x_j w_{ij} + b_i \tag{1}$$

$$y_i = f(v_i) \tag{2}$$

In Eq. (1), m denotes the number of structural elements $x_i \in \mathbf{x}$; w_{ij} and b_i denote the interconnection weight and bias between the input and hidden layer, respectively; and v_i is the sum of the weighted inputs fed into activation function f in Eq. (2). Output y_i becomes an input for the hidden layer and passes to the output layer in the same manner. The tangent sigmoid is widely accepted as an activation function in which damage recognition can be expressed as binary numbers.

The learning process suggests a training pattern and modifies the interconnection weight $\hat{\mathbf{w}}$ between adjacent layers by minimizing the norm between the target and output vectors. Thus,

$$J(\mathbf{w}) = \frac{1}{2}\|\hat{\mathbf{z}} - \mathbf{z}\| \tag{3}$$

In Eq. (3), $\mathbf{z}$ and $\hat{\mathbf{z}}$ denote the final output and initial target output vectors, respectively. In general, learning is performed by error back propagation (Van Ooyen and Nienhuis 1992), whose gradient descent is defined as

$$\Delta\mathbf{w} = -\eta\frac{\partial J}{\partial \mathbf{w}} \tag{4}$$

In Eq. (4), η denotes the gradient rate, which typically ranges between 0.01 and 0.001. The interconnection weight is updated after n iterations as follows:

$$\mathbf{w}_{n+1} = \mathbf{w}_n + \Delta\mathbf{w}_n \tag{5}$$

The iterations are repeated until the norm level is less than a predefined threshold.

2.2 NDSI

Damage index, known as DSI, uses modal parameters from both undamaged and damaged structures (Lam *et al.* 1998). The eigenvalue problem of the ith mode of a damaged structure can be expressed as follows:

$$[\mathbf{K} - \Delta\mathbf{K} - (\omega_i^2 - \Delta\omega_i^2)\mathbf{M}](\{\phi_i\} - \Delta\{\phi_i\}) = 0 \tag{6}$$

In Eq. (6), $\mathbf{K}$ and $\mathbf{M}$ denote the stiffness and mass matrices of the intact structure, respectively; ω_i and $\{\phi_i\}$ are the natural frequency and mode shape vector of the ith mode, respectively; and Δ indicates the modal parameter changes induced by the damage. The second-order terms associated with Δ are neglected, and the definition of eigenvalue problem, $[\mathbf{K} - \omega_i^2\mathbf{M}]\{\phi_i\} = 0$, is used to simplify Eq. (6) as follows:

$$-[\Delta\mathbf{K} - \Delta\omega_i^2\mathbf{M}]\{\phi_i\} - [\mathbf{K} - \omega_i^2\mathbf{M}]\Delta\{\phi_i\} = 0 \tag{7}$$

When both sides are pre-multiplied by $\{\phi_i\}^{\mathrm{T}}$, Eq. (7) becomes

$$\{\phi_i\}^{\mathrm{T}}\Delta\mathbf{K}\{\phi_i\} - \Delta\omega_i^2\{\phi_i\}^{\mathrm{T}}\mathbf{M}\{\phi_i\} = 0 \tag{8}$$

From Eq. (8), the change in ω_i^2 can be expressed by the following:

$$\Delta\omega_i^2 = \frac{\{\phi_i\}^{\mathrm{T}}\Delta\mathbf{K}\{\phi_i\}}{\{\phi_i\}^{\mathrm{T}}\mathbf{M}\{\phi_i\}} \tag{9}$$

To express $\Delta\{\phi_i\}$ in a similar manner, $\{\phi_j\}^{\mathrm{T}}$ is pre-multiplied by Eq. (7). The eigenvalue problem $\{\phi_j\}^{\mathrm{T}}\mathbf{K} = \omega_j^2\{\phi_j\}^{\mathrm{T}}\mathbf{M}$ is used, which yields

$$\{\phi_j\}^{\mathrm{T}}\Delta\mathbf{K}\{\phi_i\} + (\omega_j^2 - \omega_i^2)\{\phi_j\}^{\mathrm{T}}\mathbf{M}\Delta\{\phi_i\} = 0 \tag{10}$$

Assuming that the changes in the mode shape vector with N number of elements are a linear combination of the mode shape vectors, the following relationship can be derived as

$$\Delta\{\phi_i\} = \sum_{j=1}^{N} c_{ij}\{\phi_j\} \tag{11}$$

In Eq. (11), c_{ij} is the linear combination coefficient of the jth mode of the intact structure. $\Delta\{\phi_i\}$ in Eq. (10) is substituted by Eq. (11) and the orthogonal property, $\{\phi_j\}^{\mathrm{T}}\mathbf{M}\{\phi_i\} = 0$ (if $i \neq j$), is used to calculate the coefficient c_{ij} as follows:

$$c_{ij} = -\frac{\{\phi_j\}^{\mathrm{T}}\Delta\mathbf{K}\{\phi_i\}}{(\omega_j^2 - \omega_i^2)\{\phi_j\}^{\mathrm{T}}\mathbf{M}\{\phi_j\}} \tag{12}$$

Substituting Eq. (12) into Eq. (11) results in the expressions for the changes in the ith mode shape vector, Thus,

$$\Delta\{\phi_i\} = \sum_{j=1}^{N} -\frac{\{\phi_j\}^{\mathrm{T}}\Delta\mathbf{K}\{\phi_i\}}{(\omega_j^2 - \omega_i^2)\{\phi_j\}^{\mathrm{T}}\mathbf{M}\{\phi_j\}}\{\phi_j\} \tag{13}$$

Similar to the changes in the mode shape vector, the changes in the system stiffness matrix can be expressed using the linear combination of member stiffness matrix k_e with fractional change α_e as follows:

$$\Delta\mathbf{K} = \sum_{e=1}^{N_{ed}} \alpha_e k_e \tag{14}$$

In Eq. (14), N_{ed} denotes the number of damaged members. α_e represents the damage extent, which ranges between zero and unity and can be considered as a scalar value when a single element is damaged or almost identical damage develops in multiple elements.

Substituting Eq. (14) into Eqs. (9) and (13), and defining the ratio between the changes in the mode shape vector and eigenvalue ($\{\psi\}_i = \Delta\{\phi_i\} / \Delta\omega_i^2$) yields the following:

$$\{\psi\}_i = \frac{\sum_{j=1}^{N}\left[-\dfrac{\{\phi_j\}^{\mathrm{T}}\sum_{e=1}^{N_{ed}} k_e\{\phi_i\}}{(\omega_j^2-\omega_i^2)\{\phi_j\}^{\mathrm{T}}\mathbf{M}\{\phi_j\}}\{\phi_j\}\right]}{\dfrac{\{\phi_i\}^{\mathrm{T}}\sum_{e=1}^{N_{ed}} k_e\{\phi_i\}}{\{\phi_i\}^{\mathrm{T}}\mathbf{M}\{\phi_i\}}} \tag{15}$$

In Eq. (15), the fractional change coefficient is eliminated from this expression, and this index is named DSI. Because the damage extent parameter α_e is canceled out, DSI depends only on the damage location and not on the extent. The normalized form of DSI, namely $\{\lambda\}_i$, is introduced to express the proportional effect of DSI on a given damage as

$$\{\lambda\}_i = \frac{\{\psi\}_i}{\sum_{i=1}^{N}|\{\psi\}_i|} \tag{16}$$

The element of $\{\lambda\}_i$ is used as an input to train the ANN and to detect the damage information.

2.3 Modal identification for output-only systems

The dynamic characteristics of the constructed structures can be estimated using system identification techniques (Juang and Pappa 1985; Chang and Pakzad 2014). The identification algorithms are generally composed of three steps. (1) The types of methods, data, and sensor geometry are determined in the pre-processing step. (2) The state space model equivalent to an actual system is developed in the eigenvalue estimation. (3) The true modal parameters are distinguished from the noisy modes in the post-processing step.

The state space model expresses the equation for dynamic analysis into a discretized first order differential equation, and the outputs are expressed as follows:

$$\mathbf{x}_{i+1} = \mathbf{A}\mathbf{x}_i + \mathbf{B}\mathbf{u}_i + \mathbf{w}_i \tag{16}$$

$$\mathbf{y}_i = \mathbf{C}\mathbf{x}_i + \mathbf{D}\mathbf{u}_i + \mathbf{e}_i \tag{17}$$

In Eqs. (17) and (18), $\mathbf{x}_i$, $\mathbf{u}_i$, and $\mathbf{y}_i$ are the state, input, and output vectors at the ith time step, respectively. Coefficients $\mathbf{A}$, $\mathbf{B}$, $\mathbf{C}$, and $\mathbf{D}$ are the system matrices, which are also known as the state, input, output, and feed-through matrices, respectively. $\mathbf{w}_i$ and $\mathbf{e}_i$ are the Gaussian distributed process noise and measurement error vectors, respectively, to fit the state and output responses, and they satisfy the following relationship:

$$\mathbf{E}\left[\begin{pmatrix}\mathbf{w}_i\\ \mathbf{e}_i\end{pmatrix}\begin{pmatrix}\mathbf{w}_j^{\mathrm{T}} & \mathbf{e}_j^{\mathrm{T}}\end{pmatrix}\right] = \begin{pmatrix}\mathbf{Q} & \mathbf{S}\\ \mathbf{S}^{\mathrm{T}} & \mathbf{R}\end{pmatrix}\delta_{ij} \tag{19}$$

In Eq. (19), δ_{ij} is the Kronecker delta. Assuming that the ambient input is dominant in the system, the governing equations can be expressed using the stochastic subsystem.

$$\mathbf{x}_{i+1} = \mathbf{A}\mathbf{x}_i + \mathbf{w}_i \tag{20}$$

$$\mathbf{y}_i = \mathbf{C}\mathbf{x}_i + \mathbf{e}_i \tag{21}$$

The subspace algorithms use a projection of future output onto input/output data to estimate the transition matrices of the system (Zeiger and McEwen 1974). The numerical expression of the projection is defined as $\mathbf{P}/\mathbf{Q} = \mathbf{P}\mathbf{Q}^{\mathrm{T}}(\mathbf{Q}\mathbf{Q}^{\mathrm{T}})^{-1}\mathbf{Q}$. The numerical algorithm for subspace state space system identification (N4SID), one of the well-known subspace algorithms, uses two successive projections of the future output onto the past/future input and past output to derive the equivalent state space model. The expansion of the projection can be written as

$$\mathbf{Z}_i = [\mathbf{L}_i^1|\mathbf{L}_i^2|\mathbf{L}_i^3]\begin{bmatrix}\mathbf{U}_{0|i-1}\\ \mathbf{U}_{i|2i-1}\\ \mathbf{Y}_{0|i-1}\end{bmatrix} \tag{22}$$

In Eq. (22), $\mathbf{U}_{0|i-1}$, $\mathbf{U}_{i|2i-1}$, and $\mathbf{Y}_{0|i-1}$ are the block matrices of the past input, future input, and past output, respectively. Block coefficients $\mathbf{L}_i^1$, $\mathbf{L}_i^2$, and $\mathbf{L}_i^3$ are the functions associated with the structural properties and the covariance between the output and state vectors. The identification of the output-only system in the Structural Modal Identification Toolsuite (SMIT) assumes a zero contribution for the deterministic subsystem, which indicates that the future output is projected only on the past output.

The singular value decomposition is used to extract the transition state and output matrices. The modal parameters, equivalent to the true structure, are extracted by solving the eigenvalue problem as follows:

$$\widetilde{\mathbf{A}} = \mathbf{\Psi}\mathbf{\Lambda}\mathbf{\Psi}^{-1} \tag{23}$$

In Eq. (23), $\mathbf{\Lambda} = \mathrm{diag}(\lambda_i)$ for $i = 1,2,\ldots,N_s$, which can be converted into a continuous time domain form as

$$\mu_i = \frac{\log(\lambda_i)}{\Delta t} \tag{24}$$

The natural frequencies and damping ratios are given by

$$\omega_i = \sqrt{\mu_i \cdot \mu_i^*} \ \ (*\text{ conjugate form}) \tag{25}$$

$$\zeta_i = -\frac{Re(\mu_i)}{\omega_i} \tag{26}$$

The number of identified modesm, that is, N_s, generally exceeds the true structural modes. To eliminate the spurious computational/noise modes, a stabilization diagram is used. The ranges of the natural frequency, damping ratio, and modal phase collinearity, which represents the phase angle in the mode shape vector, are used to narrow the desirable candidates (Dorvash and Pakzad 2012; Chang 2018). The similarity thresholds of the natural frequency, damping ratio, and mode shape vector in terms of MAC between adjacent model orders are used to distinguish the true structural modes (Allemang 2003). The MAC between mode shapes $\{\phi_A\}$ and $\{\phi_B\}$ is defined as

$$\mathrm{MAC} = \frac{|\{\phi_A\}^{\mathrm{T}}\{\phi_B\}|}{\sqrt{(\{\phi_A\}^{\mathrm{T}}\{\phi_A\})(\{\phi_B\}^{\mathrm{T}}\{\phi_B\})}} \tag{27}$$

3. Development of ANN

An FE model of a three-story shear building model is developed to train for damage scenarios. Massless beam-column elements are used to define the physical structure, and a concentrated mass is assigned to each joint. The mode shapes of the intact structure are shown in Fig. 3. The physical beam and column members are composed of four elements. For the first three modes, the modal coordinates at both ends of a beam member, are almost identical in the horizontal direction. Thus, the damage is difficult to identify when one of the column members connected to the beam is damaged. To resolve this issue, a mode shape matrix for ANN is created using the modal coordinates at a quarter length of the column member apart from each joint, as shown in Fig. 4. Accordingly, the assigned column number is the same as the number of the sensing location.

In this study, damage is defined as the decrease in the stiffness of a single or two column members, wherein the amount of stiffness reduction in the two columns is assumed to be identical. A total of 21 damage patterns (6 from the damage in the single member and the rest from the damage in the combination of two members) can be generated and used to train the ANN. The NDSI of each mode is shown in Fig. 5 when the damage is assumed to be a 30 % stiffness reduction in the single column member. The bold red line in each subplot indicates the damaged column member. In general, the change in the modal coordinate is the most sensitive in the third mode. To evaluate the effect of the damage extent, the NDSI is estimated at every 20% increment in the stiffness reduction. Figure 6 shows that the NDSI is barely affected by the variation in damage extent.

ANN is composed of 3 layers and 42 neurons (18–18–6 for the input–hidden–output layers). The input is defined as the NDSI, which ranges from zero to unity, in a vector form as

$$\{input\}_{ST1} = \{\{\lambda_1\}^{\mathrm{T}} \quad \{\lambda_2\}^{\mathrm{T}} \quad \{\lambda_3\}^{\mathrm{T}}\} \tag{28}$$

To reflect the uncertainty contribution to the modal parameters for training, 100 samples of white noise with a mean of zero and standard deviation of σ, which varies from 0.05 to 0.15, are added to the natural frequencies and mode shapes. Tangent sigmoid is utilized as an activation function for both hidden and output layers. The target output is set to "+1" and "–1" for the damaged and undamaged condition of a column member, respectively. The mathematical expression for the output target vector is defined as

$$\{output\}_{ST1} = \{L_1 \quad L_2 \quad L_3 \quad L_4 \quad L_5 \quad L_6\}$$
$$\begin{cases} L_i = +1 \ if \ damaged \\ L_i = -1 \ if \ undamaged \end{cases}, \ (i = 1, \dots, 6) \tag{29}$$

A total of 2,121 scenarios (21 damage patterns × 101 noise-free and noisy cases) are used to develop the first-stage ANN. The damage level is randomly selected between 10% and 90%. The 420 samples (21 damage patterns × 20 noisy cases) are selected to identify the damage location, whereas the remainder are used for the validation. The training is performed until the error is less than 5.0×10^{-5}, which is the so-called well-trained ANN, or the iteration is more than 1,000, where, in this case, the training is considered to be unsuccessful. The presence of damage is determined by the output sign convention of ANN such that a positive output represents the existence of damage and a negative output represents no damage. The validation shows that more than 98% of the samples (1,667) identify the damage and its location.

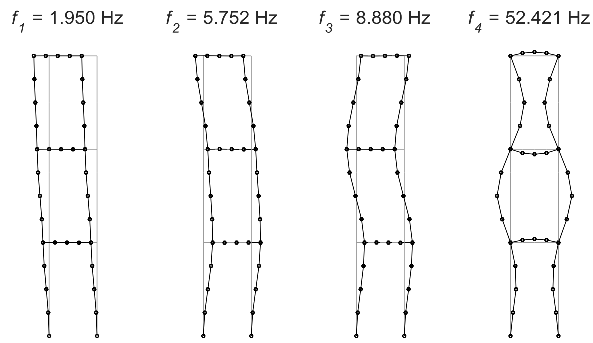

Fig. 3 First four mode shapes and natural frequencies

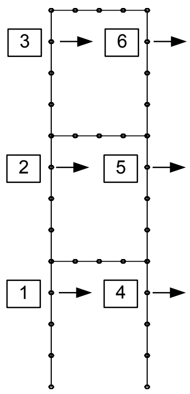

Fig. 4 Numbering of column members and sensor locations

Further simulation is performed when two columns are damaged nut to different extents. A total of 240 damage scenarios are defined when the stiffness reduction is set to 50% for a column member and varies from 10% to 90% with an interval of 10% for another damaged column. Table 1 lists the number of accurate damage identifications among the damage cases. Each damage case is simulated 30 times by varying the noise in the modal parameters. The fundamental assumption for NDSI is that the damage to multiple members is identical. Thus, ANN performs well for the damage scenarios close to this condition.

The second-stage ANN activated by the result of the previous step, evaluates the extent of damage. The mode shape vectors are used as the input for the ANN. The output target is set to the member stiffness ratio between the damaged and intact structure; for instance, the output is targeted to 0.9 when a 10% stiffness reduction occurs.

$$\{input\}_{ST2} = \{\{\phi_1\}^{\mathrm{T}} \quad \{\phi_2\}^{\mathrm{T}} \quad \{\phi_3\}^{\mathrm{T}}\} \tag{30}$$

$$\{output\}_{ST2} = \begin{cases} \alpha_e & \text{for a single column} \\ [\alpha_{e1} \quad \alpha_{e2}] & \text{for two columns} \end{cases} \tag{31}$$

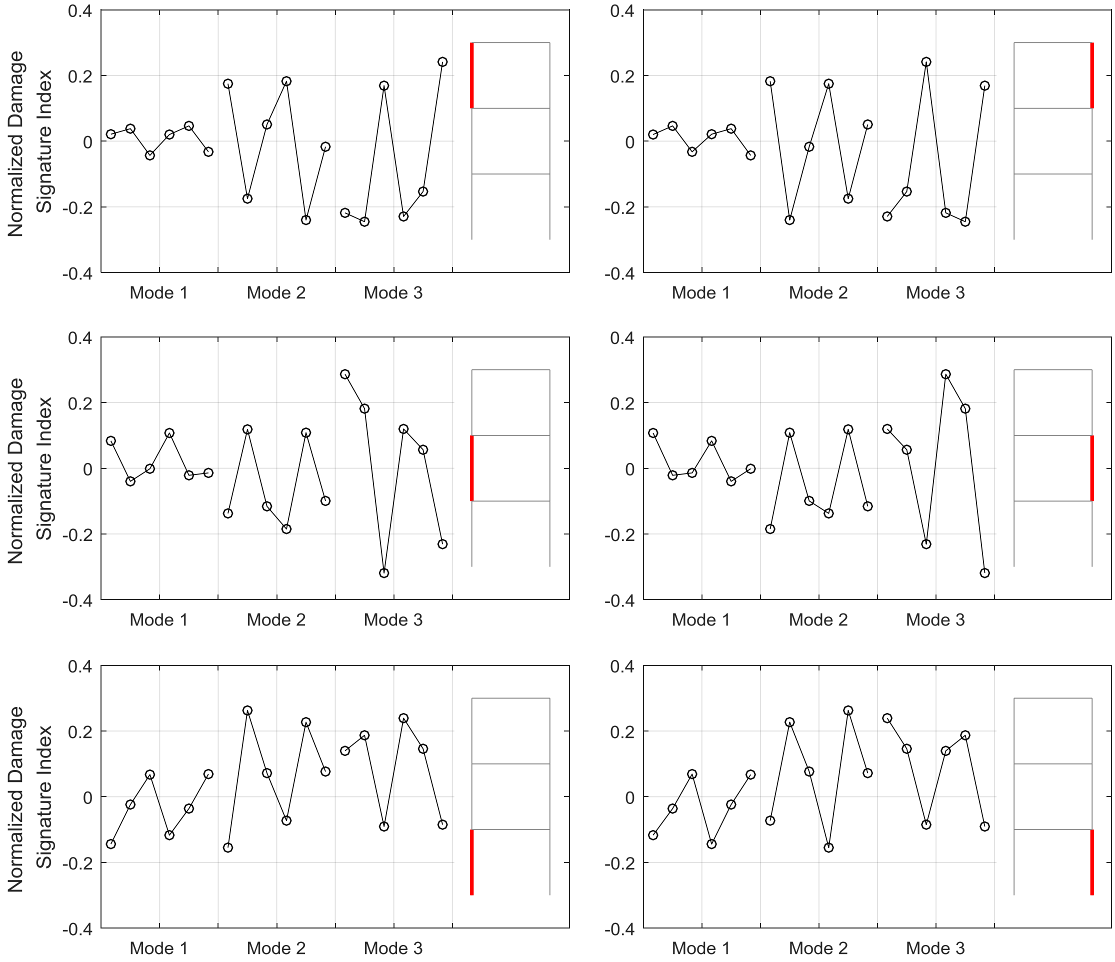

Fig. 5 NDSI for six sensing locations under a 30% stiffness reduction in each column (bold red indicates the damaged member of each subplot)

The ANN is composed of either 18–6–1 or 18–6–2 neurons for the input–hidden–output layers when a single element or two elements are damaged, respectively. The tangent sigmoid and linear transfer functions are used as activation functions for the hidden and output layers, respectively.

When a single column is damaged, a total of 909 scenarios (9 damage levels × 101 noise-free and with noisy cases) are created to train the ANN. Among them, 100 samples (5 damage levels × 20 noisy cases) are selected for the training, and the remaining 809 samples are used for the validation. Similarly, 81 damage scenarios are created when the two column members are damaged. The range of the stiffness reduction for each damage member varies from 10% to 90% with an increment of 10%. A total of 8,181 scenarios are created considering 101 noise-free and noisy cases; 1,620 samples are selected to train the ANN, and the remaining samples are used to validate the performance of the ANN.

To verify the developed algorithm, 21 damage scenarios corresponding to the damage pattern are processed for the proposed damage detection procedure. The results show good agreement in detecting the damage and its extent for all cases. The root mean square (RMS) errors between the target and damaged stiffness are listed in Table 2. The diagonal elements indicate the damage on a single column and the remaining elements indicate the equivalent damage on the two columns. The low values of RMS error, which is generally less than 0.015, demonstrate that the proposed algorithm successfully evaluates the damage extent as well as its location.

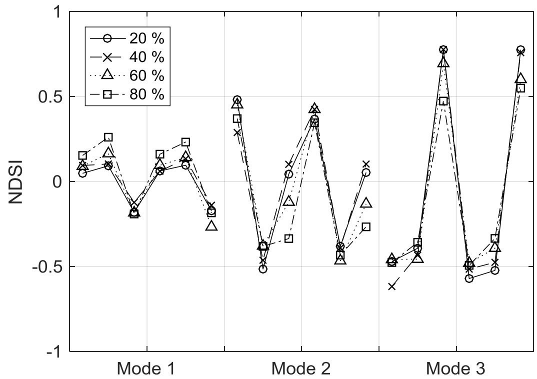

Fig. 6 NDSI for varying stiffness reduction in column 2

Table 1 Damage detection simulation when two columns are damaged

Damage scenario	Successful damage detection
50%–10%	0/30
50%–20%	6/30
50%–30%	18/30
50%–40%	30/30
50%–60%	30/30
50%–70%	21/30
50%–80%	15/30
50%–90%	12/30

Table 2 RMS error for the evaluation of damage extent when a single member or two members are damaged

Damage location	1	2	3	4	5	6
1	0.005					
2	0.0017	0.0046				
3	0.0053	0.0058	0.0097			
4	0.005	0.0105	0.003	0.0031		
5	0.0113	0.0041	0.0036	0.0023	0.0063	
6	0.0024	0.0119	0.0018	0.0019	0.0051	0.0079

4. Verification using laboratory experiment

The laboratory test using a three-story shear frame model, shown in Fig. 7, is conducted to verify the performance of the proposed method. For the intact structure, the dimensions of the column and beam are determined to be 40 mm × 3 mm × 446 mm and 40 mm × 4 mm × 246 mm, respectively (Fig. 8). Each joint is considered as a lumped mass of 666.58 g, and T-shaped connectors of 15.3 g are installed between the mass and columns or beams. The height of each story is set to 500 mm, and the length between two masses in a story is set to 300 mm.

The vibration response is measured using accelerometers attached to each floor of the shear frame model subjected to white noise excitation from a shake table. A subspace algorithm (N4SID-OO) included in SMIT (Chang and Pakzad 2014) is used to identify the mode shapes. To check the model similarity to the FE model, the discrepancy in the natural frequencies and MAC values is estimated between the eigen analysis of the FE model and identified mode shape vectors using the acceleration response (Table 3). Although the modal frequency of the first and second modes is relatively large, it can be ignored because the third modal frequency is the most effective for NDSI estimation.

Experiments are performed for three damage scenarios, that is, (a) column 2, (b) column 5, and (c) columns 1and 5 are damaged. For a given case of damage, the output of the ANN for the damage location is shown in Fig. 9. For all investigated scenarios, the damage locations are successfully identified. Although the output values for column 4 in case (a) are slightly different from "–1," the second-stage ANN is only activated for column 2. This occurs because of the continuity of the tangent sigmoid function when binary damage information is converted into the ANN output. A similar offset is observed for column 2 in case (b).

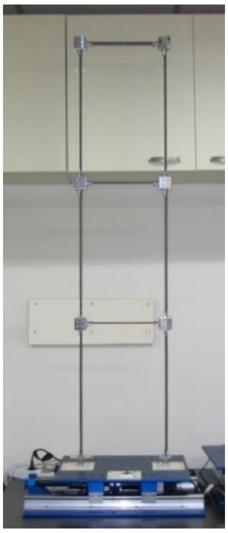

Fig. 7 Three-story shear building model for the experiment

Fig. 8 Column members (intact and damaged conditions)

Table 3 Modal parameter comparison between the FE model and three-story shear frame models

Mode	Modal Frequency (Hz)	MAC
1	0.2741	0.9974
2	0.2350	0.9989
3	0.0564	0.9987

The positive outputs from the first-stage activate the second-stage ANN for damage extent evaluation. The percentage performance of the member stiffness on the damaged elements is shown in Fig. 9. In general, the extent applied damage for a stiffness reduction of approximately 30%. The maximum difference among the investigated damage scenarios is up to 10% for column 5 in case (c).

5. Conclusions

In this study, a damage detection method using ANN is developed for a two-stage scheme, and its performance is verified via experiments on a three-story shear building model. The first ANN stage is developed to identify the

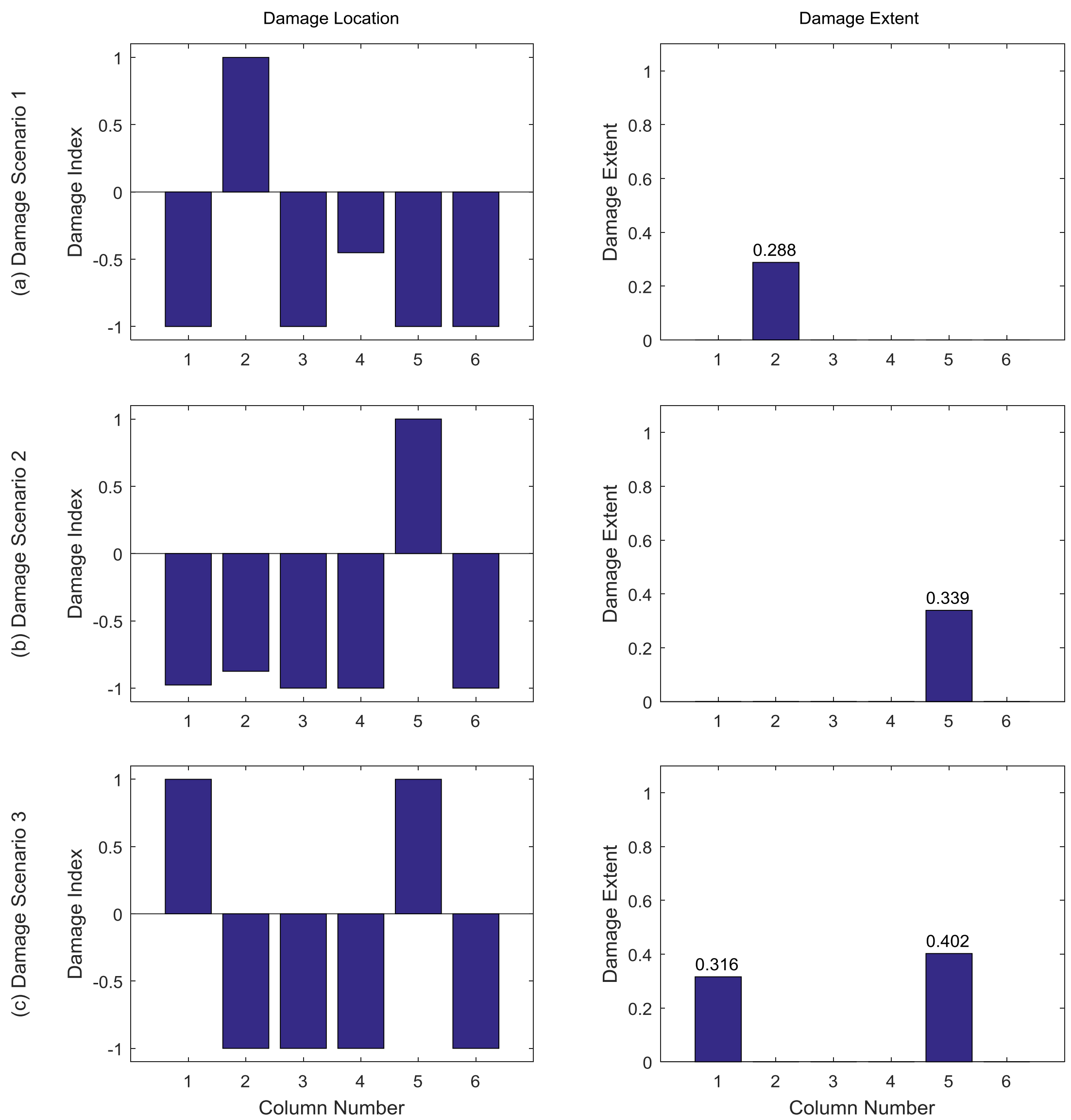

Fig. 9 Damage identification using acceleration data subjected to the white noise excitation when damage occurs in (a) column 2, (b) column 5, and (c) columns 1 and 5

presence of damage and its location, and the next ANN stage determines the damage extent. For each ANN, the algorithm is trained using the modal parameters (NDSI and identified mode shape vector) induced from the modal information. An experiment on the intact/damaged shear building model is performed to validate the effectiveness of the proposed damage detection method, and the following results are derived.

· DSI, which is the ratio between the changes in the modal frequency and the corresponding mode shape, is developed by artificially generated damage. The mathematical expression of DSI shows that it is only dependent on the damage location and the damage extent is irrelevant to it. For the training process, DSI is normalized using the investigated modes.

· The two-stage scheme improves the computation efficiency of the training by splitting the damage detection into the identification of damage location and its extent. Considering the complexity of the FE model for civil infrastructure and the greater amount of modal information associated with it, only a few computations improve the performance of the ANN compared to the single-stage scheme, when it is applied to existing structures.

· A subspace algorithm is employed to identify the modal parameters from the measured data. N4SID-OO in SMIT is utilized to capture the modal parameters under the assumption that the stochastic contribution is dominant on the measured response. The MAC values between the mode shape vectors from the FE model and the measured response are used to compare the suitability of using the FE model for the ANN.

· The proposed method successfully identifies the damage information. The two-stage scheme of the ANN is sequentially activated and accurately detects both the damage location and extent for all investigated damage scenarios.

Acknowledgments

This research was supported by a grant from the R&D Program of the Korea Railroad Research Institute and the Korea Construction Engineering Development Collaboratory Program Management Center (KOCED PMC) at Seoul National University, Republic of Korea. The authors wish to express their gratitude for the financial support.

The first and third authors express special thanks to Professor Jae Kwan Kim for his lifelong devotion to the development of civil engineering in Korea.

References

Ali, J.B., Fnaiech, N., Saidi, L., Chebel-Morello, B. and Fnaiech, F. (2015), "Application of empirical mode decomposition and artificial neural network for automatic bearing fault diagnosis based on vibration signals", *Appl. Acoust.*, **89**, 16-27. https://doi.org/10.1016/j.apacoust.2014.08.016.

Allemang, R.J. (2003), "The modal assurance criterion-twenty years of use and abuse", *Sound Vib.*, **37**(8), 14-23.

Bakhary, N., Hao, H. and Deeks, A.J. (2010), "Structure damage detection using neural network with multi-stage substructuring", *Adv. Struct. Eng.*, **13**(1), 95-110. https://doi.org/10.1260/1369-4332.13.1.95

Cha, Y.J., Choi, W. and Büyüköztürk, O. (2017), "Deep learning-based crack damage detection using convolutional neural networks", *Comput. Aided Civ. Infrastruct. Eng.*, **32**(5), 361-378. https://doi.org/10.1111/mice.12263.

Chang, M. (2018), "Application studies on structural modal identification toolsuite for seismic response of shear frame structure", *J. Earthq. Eng. Soc. Korea*, **22**(3), 201-210.

Chang, M., Maguire, M. and Sun, Y. (2017), "Framework for mitigating human bias in selection of explanatory variables for bridge deterioration modeling", *J. Infrastruct. Sys.*, **23**(3), 04017002. https://doi.org/10.5000/EESK.2018.22.3.201.

Chang, M. and Pakzad, S.N. (2014), "Observer Kalman filter identification for output-only systems using interactive structural modal identification toolsuite", *J. Bridge Eng.*, **19**(5), 04014002. https://doi.org/10.1061/(ASCE)BE.1943-5592.0000530.

Chang, P.C., Flatau, A. and Liu, S.C. (2003), "Health monitoring of civil infrastructure", *Struct. Health Monit.*, **2**(3), 257-267. https://doi.org/10.1177/1475921703036169.

Chen, J.D. and Loh, C.H. (2018), "Two-stage damage detection algorithms of structure using modal parameters identified from recursive subspace identification", *Earthq. Eng. Struct. Dyn.*, **47**(3), 573-593. https://doi.org/10.1002/eqe.2980.

Cho, H.N., Choi, Y.M., Lee, S.C., and Hur, C.K. (2004), "Damage assessment of cable stayed bridge using probabilistic neural network", *Struct. Eng. Mech.*, **17**(3-4), 483-492. http://doi.org/10.12989/sem.2004.17.3_4.483.

Cornwell, P., Doebling, S.W. and Farrar, C.R. (1999), "Application of the strain energy damage detection method to plate like structures", *J Sound Vib.*, **224**(2), 359- 374. https://doi.org/10.1006/jsvi.1999.2163.

Dorafshan, S., Thomas, R.J. and Maguire, M. (2018), "Comparison of deep convolutional neural networks and edge detectors for image-based crack detection in concrete", *Constr. Build. Mater.*, **186**, 1031-1045. https://doi.org/10.1016/j.conbuildmat.2018.08.011.

Dorvash, S. and Pakzad, S.N. (2012), "Effects of measurement noise on modal parameter identification", *Smart Mater. Struct.*, **21**(6), 065008. https://doi.org/10.1088/0964-1726/21/6/065008.

Farreras-Alcover, I., Chryssanthopoulos, M.K. and Andersen, J.E. (2015), "Regression models for structural health monitoring of welded bridge joints based on temperature, traffic and strain measurements", *Struct. Health Monit.*, **14**(6), 648-662. https://doi.org/10.1177%2F1475921715609801.

Hakim, S.J.S., Noorzaei, J., Jaafar, M.S., Jameel, M. and Mohammadhassani, M. (2011), "Application of artificial neural networks to predict compressive strength of high strength concrete", *Int. J. Phys. Sci.*, **6**(5), 975-981. https://doi.org/10.5897/IJPS11.023.

Hakim, S.J.S. and Razak, H.A. (2014), "Modal parameters based structural damage detection using artificial neural networks-a review", *Smart Struct. Sys.*, **14**(2), 159-189. http://dx.doi.org/10.12989/sss.2014.14.2.159.

Juang, J.N. and Pappa, R.S. (1985), "An eigensystem realization algorithm for modal parameter identification and model reduction", *J. Guid., Control, Dyn.*, **8**(5), 620-627. https://doi.org/10.2514/3.20031.

Ko, J.M., Sun, Z.G. and Ni, Y.Q. (2002), "Multi-stage identification scheme for detecting damage in cable-stayed Kap Shui Mun Bridge", *Eng. Struct.*, **24**(7), 857-868. https://doi.org/10.1016/S0141-0296(02)00024-X.

Kondo, I. and Hamamoto, T. (1994), "Local damage detection of flexible offshore platforms using ambient vibration measurement", *Int. Soc. Offshore Polar Eng.*, **4**, 400-407.

Lam, H.F., Ko, J.M. and Wong, C.W. (1998), "Localization of damaged structural connections based on experimental modal and sensitivity analysis", *J. Sound Vib.*, **210**(1), 91-115. https://doi.org/10.1006/jsvi.1997.1302.

Lee, J.J., Lee, J.W., Yi, J.H., Yun, C.B. and Jung, H.Y. (2005), "Neural networks-based damage detection for bridges considering errors in baseline finite element models", *J. Sound Vib.*, **280**(3-5), 555-578. https://doi.org/10.1016/j.jsv.2004.01.003

Levin, R.I. and Lieven, N.A.J. (1998), "Dynamic finite element model updating using neural networks", *J. Sound Vib.*, **210**(5), 593-607. https://doi.org/10.1006/jsvi.1997.1364.

Limongelli, M.P. (2010), "Frequency response function interpolation for damage detection under changing environment", *Mech. Sys. Signal Process.*, **24**(8), 2898-2913. https://doi.org/10.1016/j.ymssp.2010.03.004.

Magalhães, F., Cunha, A. and Caetano, E. (2012), "Vibration based structural health monitoring of an arch bridge: from automated OMA to damage detection", *Mech. Sys. Signal Process.*, **28**, 212-228. https://doi.org/10.1016/j.ymssp.2011.06.011.

Maguire, M., Roberts-Wollmann, C. and Cousins, T. (2018), "Live-load testing and long-term monitoring of the Varina-Enon Bridge: Investigating thermal distress", *J. Bridg. Eng.*, **23**(3), 04018003. https://doi.org/10.1061/(ASCE)BE.1943-5592.0001200.

Majumdar, A., De, A., Maity, D. and Maiti, D.K. (2013), "Damage assessment of beams from changes in natural frequencies using ant colony optimization", *Struct. Eng. Mech.*, **45**(3), 391-410. https://doi.org/10.12989/sem.2013.45.3.391.

Nguyen, V.H., Schommer, S., Maas, S. and Zürbes, A. (2016), "Static load testing with temperature compensation for structural health monitoring of bridges", *Eng. Struct.*, **127**, 700-718. https://doi.org/10.1016/j.engstruct.2016.09.018.

Pandey, A.K., Biswas, M. and Samman, M.M. (1991), "Damage detection from changes in curvature mode shapes", *J. Sound Vib.*, **145**(2), 321-332. https://doi.org/10.1016/0022-460X(91)90595-B.

Park, J.H., Kim, J.T., Hong, D.S., Ho, D.D. and Yi, J.H. (2009), "Sequential damage detection approaches for beams using time-modal features and artificial neural networks", *J. Sound Vib.*, **323**(1-2), 451-474. https://doi.org/10.1016/j.jsv.2008.12.023.

Qu, W.L., Chen, W., and Xiao, Y.Q. (2003), "A two-step approach for joint damage diagnosis of framed structures using artificial neural networks", *Struct. Eng. Mech.*, **16**(5), 581-595. http://doi.org/10.12989/sem.2003.16.5.581.

Radzieński, M., Krawczuk, M. and Palacz, M. (2011), "Improvement of damage detection methods based on experimental modal parameters", *Mech. Sys. Signal Process.*, **25**(6), 2169-2190. https://doi.org/10.1016/j.ymssp.2011.01.007.

Ratcliffe, C.P. (1997), "Damage detection using a modified Laplacian operator on mode shape data", *J. Sound Vib.*, **204**(3), 505-517. https://doi.org/10.1006/jsvi.1997.0961.

Salawu, O.S. (1997), "Detection of structural damage through changes in frequency: A review", *Eng. Struct.*, **19**(9), 718-723. https://doi.org/10.1016/S0141-0296(96)00149-6.

Shahidi, S.G. and Pakzad, S.N. (2013), "Generalized response surface model updating using time domain data", *J. Struct. Eng.*, **140**(8), A4014001. https://doi.org/10.1061/(ASCE)ST.1943-541X.0000915.

Sohn, H. (2007), "Effects of environmental and operational variability on structural health monitoring", *Philos. Trans. R. Soc. Lond. A: Math., Phys. Eng. Sci.*, **365**(1851), 539-560. https://doi.org/10.1098/rsta.2006.1935.

Sohn, H., Farrar, C.R., Hemez, F.M., Shunk, D.D., Stinemates, D.W., Nadler, B.R. and Czarnecki, J.J. (2003), "A review of structural health monitoring literature: 1996–2001", LA-UR-02-2095; Los Alamos National Laboratory, USA.

Torres, V., Zolghadri, N., Maguire, M., Barr, P. and Halling, M. (2018), "Experimental and analytical investigation of live-load distribution factors for double tee bridges", *J. Perform. Constr. Facil.*, **33**(1), 04018107. https://doi.org/10.1061/(ASCE)CF.1943-5509.0001259.

Van Ooyen, A. and Nienhuis, B. (1992), "Improving the convergence of the back-propagation algorithm", *Neural Netw.*, **5**(3), 465-471. https://doi.org/10.1016/0893-6080(92)90008-7.

Worden, K. and Manson, G. (2006), "The application of machine learning to structural health monitoring", *Philos. Trans. Royal Soc. A: Math., Phys. Eng. Sci.*, **365**(1851), 515-537. https://doi.org/10.1098/rsta.2006.1938.

Wu, X., Ghaboussi, J. and Garrett Jr, J.H. (1992), "Use of neural networks in detection of structural damage", *Comput. Struct.*, **42**(4), 649-659. https://doi.org/10.1016/0045-7949(92)90132-J.

Yazdanpanah, O., Seyedpoor, S.M., and Akbarzadeh Bengar, H. (2015). "A new damage detection indicator for beams based on mode shape data", *Struct. Eng. Mech.*, **53**(4), 725-744. http://doi.org/10.12989/sem.2015.53.4.725.

Yoon, M.K., Heider, D., Gillespie Jr, J.W., Ratcliffe, C.P. and Crane, R.M. (2005), "Local damage detection using the two-dimensional gapped smoothing method", *J Sound Vib.*, **279**(1-2), 119-139. https://doi.org/10.1016/j.jsv.2003.10.058.

Yun, C.B., Yi, J.H. and Bahng, E.Y. (2001), "Joint damage assessment of framed structures using a neural networks technique", *Eng. Struct.*, **23**(5), 425-435. https://doi.org/10.1016/S0141-0296(00)00067-5.

Zeiger, H.P. and McEwen, A. (1974), "Approximate linear realizations of given dimension via Ho's algorithm", *IEEE Trans. on Autom. Control*, **19**(2), 153-153. http://doi.org/ https://doi.org/10.1109/TAC.1974.1100525.

Zolghadri, N., Halling, M.W. and Barr, P.J. (2016), "Effects of temperature variations on structural vibration properties", *Geotechnical and Structural Engineering Congress 2016*, 1032-1043, Phoenix, USA, February. https://doi.org/10.1061/9780784479742.087.

CC